



Original article

Synthesis and biological evaluation of novel 3,4-diaryl-1,2,5-selenadiazol analogues of combretastatin A-4



Qi Guan^a, Fushan Yang^a, Dandan Guo^b, Jingwen Xu^b, Mingyang Jiang^a, Chunjiang Liu^b, Kai Bao^{a,c}, Yingliang Wu^{b,**}, Weige Zhang^{a,*}

^a Key Laboratory of Structure-Based Drug Design and Discovery, Ministry of Education, Shenyang Pharmaceutical University, 103 Wenhua Road, Shenhe District, Shenyang 110016, China

^b Department of Pharmacology, Shenyang Pharmaceutical University, 103 Wenhua Road, Shenhe District, Shenyang 110016, China

^c Division of Hematology/Oncology, Department of Medicine, Beth Israel Deaconess Medical Center and Harvard Medical School, Boston, MA 02215, USA

ARTICLE INFO

Article history:

Received 5 August 2014

Received in revised form

30 August 2014

Accepted 12 September 2014

Available online

Keywords:

Synthesis

Anti-proliferative activity

Tubulin

Combretastatin A-4

3,4-Diaryl-1,2,5-selenadiazol

Molecular modelling

ABSTRACT

A set of novel selenium-containing heterocyclic analogues of combretastatin A-4 (CA-4) have been designed and synthesised using a rigid 1,2,5-selenadiazole as a linker to fix the *cis*-orientation of ring-A and ring-B. All of the target compounds were evaluated for their *in vitro* anti-proliferative activities. Among these compounds, compounds **3a**, **3i**, **3n** and **3q** exhibited superior potency against different tumour cell lines with IC₅₀ values at the nanomolar level. Moreover, compound **3n** significantly induced cell cycle arrest in the G₂/M phase, inhibited tubulin polymerisation into microtubules and caused microtubule destabilisation. A molecular modelling study of compound **3n** was performed to elucidate its binding mode at the colchicine site in the tubulin dimer and to provide a basis for the further structure-guided design of novel CA-4 analogues.

© 2014 Elsevier Masson SAS. All rights reserved.

1. Introduction

Microtubules, the cytoskeletal polymers of α - and β -tubulin heterodimers, have an essential role in vital cellular functions, such as motility, division, shape maintenance and intracellular transport [1,2]. Interfering with either the assembly or disassembly of microtubules and spindle poisons arrests dividing cells in the G₂/M phase of the cell cycle to result mitotic catastrophe and finally apoptotic cell death [1,3]. Therefore, anticancer therapy based on microtubule targeting agents (MTAs) is receiving growing attention in drug discovery [4,5]. MTAs are known to interact with tubulin via at least four binding sites: the laulimalide, taxane (stabilisers of the microtubules), vinca alkaloid and colchicine sites (destabilisers of the microtubules). Given the success of taxanes and vinca alkaloids, which have established tubulin as a valid target in cancer therapy, research efforts have been focused on developing colchicine binding site agents for cancer treatment [6].

Combretastatin A-4 (**1a**, Fig. 1) is a natural product that was first extracted from the bark of the South African willow tree *Combretum caffrum* in 1989 and inhibits tubulin polymerisation by interacting with the colchicine binding site on tubulin [7–9]. This *cis*-stilbene shows potent cytotoxicity against a broad spectrum of human cancer cell lines, including multidrug resistant cancer cell lines [10]. Its soluble prodrug CA-4P (**1b**, Fig. 1) is currently under Phase II/III clinical evaluation in the USA as an agent used in combination treatment for various multidrug resistant solid tumours. Because of the structural simplicity of CA-4 (**1a**), large structure-activity relationships (SARs) studies of this compound and its analogues have been carried out by numerous academic and industrial groups [10,11]. SAR studies have demonstrated that the *cis*-orientation of the double bond and the presence of a 3,4,5-trimethoxyphenyl as ring-A are fundamental requirements for potent cytotoxicity [10]. Unfortunately, CA-4 (**1a**) and other olefinic analogues are prone to isomerisation into their inactive *trans*-forms during storage and administration. To avoid the stability problems of CA-4 (**1a**), suitable conformationally restricted rings, such as heterocyclic rings, have been used in place of the olefin group between ring-A and ring-B [12–14]. In 2005, G. Sorba and co-workers reported that the

* Corresponding author.

** Corresponding author.

E-mail addresses: yingliang_1016@163.com (Y. Wu), zhangweige2000@sina.com (W. Zhang).

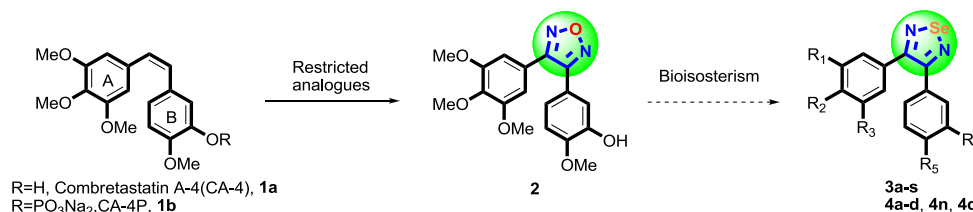


Fig. 1. Combretastatin A-4 (CA-4, **1a**), its water-soluble derivate (CA-4P, **1b**), furazan analogue (**2**) and general structure of the target compounds.

cis-locked analogue (**2**, Fig. 1) of CA-4 embodying a furazan ring exhibited very potent antitumour activity [15].

Recently, the application of organoselenium compounds in cancer prevention and treatment has become a fascinating field [16–19]. A large body of evidence shows that selenium effectively inhibits tumourigenesis in both animal models and epidemiological studies [19]. As shown in Fig. 1, we hope that the isosteric substitution of the oxygen atom in the furazan ring by selenium retains the structural features required for its potent activity. In this study, we report the synthesis, biological evaluation and the preliminary SARs of 3,4-diaryl-1,2,5-selenadiazole analogues of CA-4.

2. Results and discussion

2.1. Chemistry

The synthetic methods for the preparation of target compounds are summarised as follows (Scheme 1). In this synthetic work, we opted for a synthetic route that involves an initial umpolung of the substituted benzaldehydes **5** or **6** via transformation to their corresponding α -hydroxyphosphonates **7** or **8**. Next, the hydroxyl group was protected by 3,4-dihydro-2H-pyran (THP), followed by a Horner-Wadsworth-Emmons (HWE)-type reaction with a suitable second benzaldehyde, yielding deoxybenzoins **11a–g** and **12a–d** [14,20]. Compounds **13a–g** and **14a–d** were synthesised in a microwave (MW) reactor by treating the appropriate deoxybenzoin with selenium(IV) oxide in dimethylsulphoxide (DMSO) at 150 °C (150 W) for 2 min, and the following transformations into dioxime **15a–g** and **16a–d** were performed in an excess of hydroxylamine hydrochloride and pyridine in refluxing ethanol for 3 days [15,21]. These intermediates were then directly used for the next step to furnish the desired 1,2,5-selenadiazoles **3a–l** and **4a–d** upon dehydrating with selenium(IV) oxide in refluxing *N,N*-dimethylformamide (DMF) [22]. Subsequently, the deprotection of **3b**, **3e–g** and **4b** with AlCl_3 afforded **3m–p** and **4n** at yields of 75–89% [23], and the amino-substituted **3q**, **3r** and **4q** were obtained by reducing the nitro group of **3c**, **3h** and **4c** in a refluxing $\text{Fe}(\text{OH})_2$ solution [24]. Finally, **3q** was alkylated with methyl iodide in DMF to provide **3s**.

2.2. Biological evaluation

2.2.1. In vitro anti-proliferative activity

In an attempt to evaluate the ability of various 3,4-diaryl-1,2,5-selenadiazole derivatives to inhibit cancer cells, the target compounds **3a–e**, **3i–s**, **4a**, **4c**, **4d**, **4n**, **4q** and reference compound CA-4 (**1a**) were screened for anti-proliferative activity against three human cancer cell lines (gastric adenocarcinoma SGC-7901 cells, fibrosarcoma HT-1080 cells, and mouth epidermal carcinoma KB cells) using a standard MTT assay (Table 1). The reported IC_{50} values are the average of at least three independent experiments.

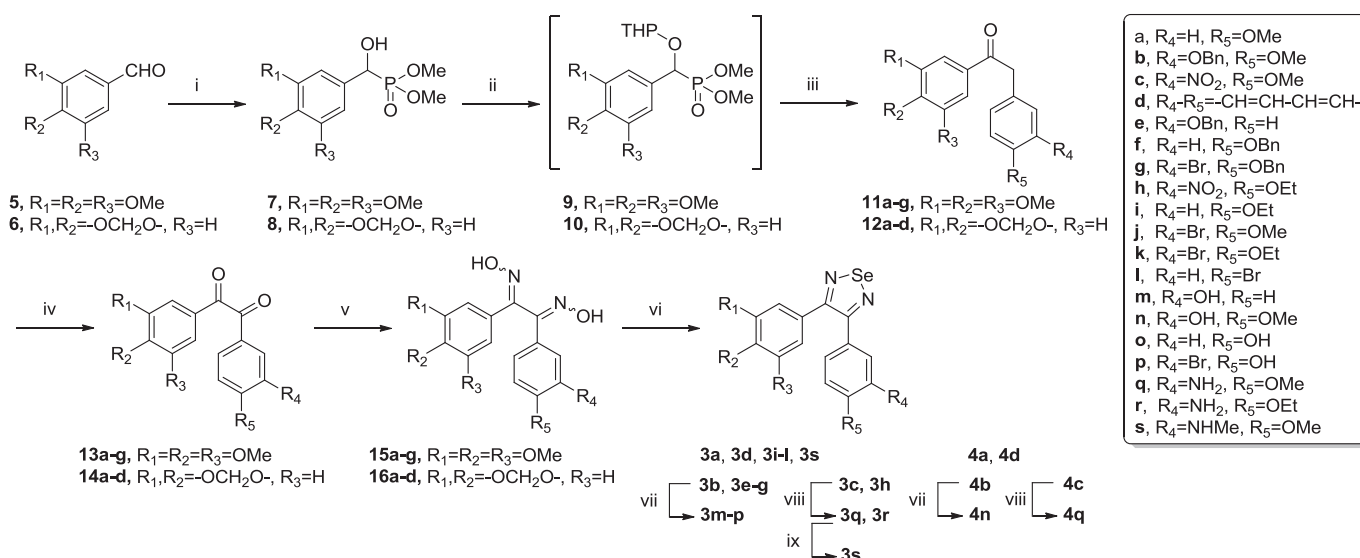
As illustrated in Table 1, most of the target compounds showed moderate-to-excellent anti-proliferative activity against different cancer cells, with potencies in the single-digit μM range, indicating that the introduction of the 1,2,5-selenadiazole moiety as a suitable mimic for the *cis*-olefin present in CA-4 (**1a**) maintained potent anti-proliferative activity. A comparison of compounds **3a**, **3i**, **3l** and **3o** revealed a substitution effect at C4 of ring-B. Compound **3a**, which contains a methoxy group, showed the most potent activity against SGC-7901, HT-1080 and KB cells, with IC_{50} values of 0.063, 0.084 and 0.031 μM , respectively. The conversion of the 4-OMe to 4-OEt (**3i**) resulted in a 5–12-fold decrease in potency. When the 4-Br and 4-OH were incorporated, the anti-proliferative activities of compounds **3l** and **3o** were almost lost. In the ring-B modification, additional $-\text{NH}_2$ and $-\text{OH}$ groups accompanied by a 4-OMe were found to improve the biological activity. However, compound **3c**, which contains a nitro group accompanied by a 4-OMe group, displayed a dramatic decrease in its biological activity, indicating that the electron-withdrawing NO_2 group is disfavoured. A similar phenomenon was observed for compound **3j**, which contains a bromine atom at the C3 position. The addition of an extra benzyl group or methyl group, as in compound **3b** or **3s**, led to decrease in biological activity. Moreover, switching ring-B from 3-amino-4-methoxyphenyl (**3n**) to β -naphthalene (**3d**) resulted in a significant loss of activity. When ring-A was replaced with a 3,4-methylenedioxyphenyl, compounds **4a**, **4c**, **4d**, **4n** and **4q** showed much lower activities. Consequently, this finding indicates that the combination of the 3,4,5-trimethoxyphenyl with the 3-hydroxy-4-methoxyphenyl (or 3-amino-4-methoxyphenyl) is the most favourable modification for the anti-proliferative activity of 3,4-diaryl-1,2,5-selenadiazole analogues.

2.2.2. Inhibition of tubulin polymerisation

To confirm that the anti-proliferative activities of these compounds were related to the microtubule system, compound **3n**, one of the most active compounds in this series of CA-4 analogues, was evaluated for its inhibition of tubulin polymerisation (Fig. 2). Compound **3n** exhibited antitubulin activity, with an IC_{50} value of 2.89 μM , which is slightly less potent than that of CA-4 ($\text{IC}_{50} = 0.93 \mu\text{M}$). Furthermore, compound **3n** inhibited the polymerisation of tubulin in a concentration-dependent manner (Fig. 2). Treatment with 1, 2, 4 and 8 μM of compound **3n** inhibited tubulin polymerisation by 20.4%, 48.83%, 65.0% and 97.6%, respectively.

2.2.3. Analysis of immunofluorescence staining

In an attempt to further identify the cellular changes that may be relevant to the anti-proliferative activity of compound **3n**, we evaluated its effect on the microtubule network via tubulin immunostaining. A microscopic analysis of HT-1080 cells stained with α -tubulin antibodies demonstrated a well organised microtubular network in control cells (Fig. 3). As visualised in Fig. 3 and similar to CA-4 (**1a**), compound **3n** at a concentration that was twice the IC_{50}



Scheme 1. Reagents and conditions: (i) Dimethyl phosphite, NaOMe, MeOH, 50 °C; (ii) TsOH cat., 3,4-dihydro-2H-pyran (THP), anhydrous toluene, under N₂ atmosphere, 50 °C; (iii) (a) *n*-BuLi, anhydrous THF, -55 °C; (b) Substituted benzaldehydes, anhydrous THF, -55–0 °C; (c) HCl aq. (12 M), MeOH, rt.; (iv) Selenium(IV) oxide, DMSO, microwave, 150 °C, 150 W, 2 min; (v) NH₂OH·HCl in Py/EtOH, 90 °C; (vi) Selenium(IV) oxide, DMF, reflux; (vii) AlCl₃, CH₂Cl₂, 0 °C; (viii) Fe(OH)₂, reflux; (ix) MeI, K₂CO₃, DMF, 60 °C.

significantly impacted the microtubule network in HT-1080 cells and induced cell rounding, detachment, and a loss of the radial distribution of structured microtubules. These results indicate that compound **3n** can destabilise microtubules.

2.2.4. Cell cycle analysis

Because the inhibition of tubulin polymerisation is often implicated in G₂/M phase arrest in various cancer cell lines, the effect of compound **3n** at various concentrations on cell cycle progression was investigated in HT-1080 cells via flow cytometry (Fig. 4). The effect of CA-4 (**1a**) on the cell cycle of HT-1080 cells was also comparatively examined as a positive control. After 24 h of exposure, compound **3n** was found to obviously increase the percentage of cells in the G₂/M and sub-G₁ phases, with a concomitant decrease in cells in the G₀/G₁ and S phases. Compound **3n** was demonstrated to clearly cause significant G₂/M phase arrest in a concentration-dependent manner, which was consistent with the behaviour of CA-4 (**1a**), the tubulin-binding agent.

2.3. Molecular modelling

To better understand the interactions between the newly synthesised compounds and tubulin, the potential binding mode of compound **3n**, a highly potent compound, at the colchicine site in the tubulin dimer was investigated by using the CDocker program in the Discovery Studio 3.0 software with the tubulin crystal structure (PDB: 1SA0) [25,26], as in our previous study. To compare the binding features of compound **3n** with CA-4 (**1a**), both compounds were docked into tubulin. In the binding models shown in Fig. 5A, the binding orientations of compound **3n** (purple) and CA-4 (orange) superimposed well with each other and with DAMA-colchicine (cyan), the ligand used in the tubulin crystal structure. As evident in Fig. 5A, a hydrogen bond is present between Val α 181 in the α -T5 loop of tubulin and the hydroxyl group on ring-B of compound **3n** and CA-4 (**1a**). This hydrogen bond is also observed between Val α 181 and the carbonyl group on ring-C of DAMA-colchicine. In addition, the trimethoxybenzene rings of these compounds are well overlapped with each other, and hydrogen bonds formed between the oxygen of two methoxyl groups and the key residue Cys β 241 in the active site. The results of the

computational modelling analysis further support the results of the inhibition of tubulin polymerisation: compound **3n** does bind to the colchicine-binding site of microtubules.

3. Conclusion

To the best of our knowledge, we designed and synthesised new selenium-containing heterocyclic analogues of CA-4 for the first time; this process involved a rigid 1,2,5-selenadiazole as linker to fix the *cis*-orientations of ring-A and ring-B. Of these compounds, compounds **3a**, **3i**, **3n** and **3q** exhibited excellent anti-proliferative activities with IC₅₀ values at the nanomolar level, especially compounds **3n** and **3q**, which were more potent than the standard CA-4 (**1a**). The *in vitro* immunofluorescence staining and tubulin polymerisation assay demonstrated that compound **3n**, similar to CA-4 (**1a**), inhibited tubulin polymerisation into microtubules and caused microtubule destabilisation, which suggests that compound **3n** acts as a microtubule destabiliser by disrupting tubulin-microtubule dynamics. Furthermore, a flow cytometric study showed that compound **3n** significantly induced cell cycle arrest in the G₂/M phase in HT-1080 cells. A docking study was then performed and offered some insights into the further modification of the target compounds. In summary, this work not only widens the exploration of olefin modification but also provides a series of useful analogues of CA-4 (**1a**) that are potent anti-proliferative agents.

4. Experimental

4.1. Chemistry

4.1.1. General

Unless otherwise noted, all materials were obtained from commercially available sources and were used without purification. The reaction process was monitored by TLC with silica gel plates (thickness 250 μ m, Indicator F-254) under UV light. The products were purified using column chromatography (60 \AA , 200–300 mesh, Qingdao Ocean Chemicals) or silica gel plates (0.25 mm layer, Qingdao Ocean Chemicals) with the designated solvents. The melting points were measured on a hot-stage microscope (X-4,

Table 1
In vitro anti-proliferative activities of the target compounds as measured with MTT test in three human tumour cell lines.

Compound	IC ₅₀ (μM) ± SD ^a		
	SGC-7901	HT-1080	KB
3a	0.063 ± 0.007	0.084 ± 0.002	0.031 ± 0.005
3b	>30	>30	>30
3c	>30	24.78 ± 0.04	10.10 ± 0.03
3d	2.35 ± 0.44	1.11 ± 0.25	0.77 ± 0.16
3e	>30	>30	10.73 ± 0.17
3i	0.23 ± 0.04	0.16 ± 0.01	0.42 ± 0.03
3j	>30	2.59 ± 0.18	3.06 ± 0.24
3k	12.79 ± 0.51	3.46 ± 0.32	0.93 ± 0.02
3l	10.87 ± 0.32	7.40 ± 0.27	7.86 ± 0.14
3m	>30	5.98 ± 0.33	>30
3n	0.019 ± 0.002	0.021 ± 0.006	0.0039 ± 0.0003
3o	>30	14.98 ± 0.13	15.81 ± 0.05
3p	>30	16.40 ± 0.83	4.80 ± 0.47
3q	0.021 ± 0.005	0.026 ± 0.008	0.011 ± 0.002
3r	0.14 ± 0.04	10.09 ± 0.22	0.099 ± 0.013
3s	>30	0.98 ± 0.01	1.52 ± 0.02
4a	8.28 ± 0.46	>30	5.21 ± 0.48
4c	>30	>30	>30
4d	17.33 ± 0.16	23.31 ± 0.39	10.37 ± 0.21
4n	3.68 ± 0.24	0.73 ± 0.05	2.38 ± 0.11
4q	>30	13.54 ± 0.14	1.87 ± 0.07
1a^b	0.028 ± 0.003	0.0076 ± 0.0010	0.013 ± 0.002

Bold values show the IC₅₀ values of target compounds that are lower than those of the positive control CA-4 (**1a**).

^a IC₅₀: Concentration of the compound (μM) producing 50% cell growth inhibition after 72 h of drug exposure, as determined by the MTT assay. Each experiment was carried out in triplicate.

^b Used as a positive control.

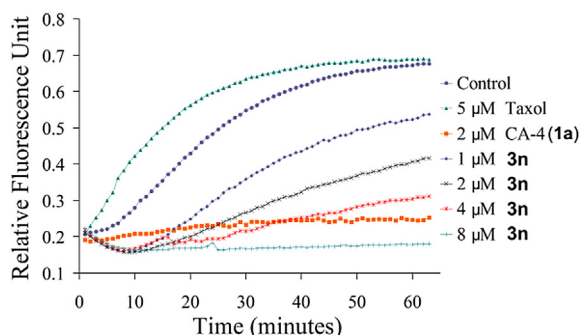


Fig. 2. Effects of **3n** on tubulin polymerisation. Tubulin had been pre-incubated for 1 min with **3n** at 1 μM, 2 μM, 4 μM and 8 μM, CA-4 at 2 μM, taxol at 5 μM or vehicle DMSO at room temperature before GTP was added to start the tubulin polymerisation reactions. The reaction was monitored at 37 °C. Taxol and CA-4 were included as positive controls.

Beijing Taike Ltd.) and are uncorrected. Mass spectra (MS) were measured on an Agilent 1100-sl mass spectrometer with an electrospray ionisation source from Agilent Co. Ltd. High resolution accurate mass determinations (HRMS) for all final target compounds were obtained on a Bruker Micromass Time of Flight mass spectrometer equipped with electrospray ionisation (ESI). NMR spectra were obtained on a Bruker AVANCE 400 (¹H, 300 MHz) and Bruker AVANCE 600 (¹³C, 150 MHz) in CDCl₃ or DMSO-*d*₆ (internal standard tetramethylsilane).

4.1.2. Synthesis of α -hydroxyphosphonates **7** and **8**

A solution of an appropriate benzaldehyde (0.1 mol), dimethyl phosphite (0.12 mol), and sodium methoxide (0.015 mol) in anhydrous methanol (25 mL) was vigorously stirred for 3 h at 50 °C. The solvent was then removed under reduced pressure and extracted

with ethyl acetate (100 mL × 3). The combined organic layer was washed with water and brine and then dried over Na₂SO₄, filtered and concentrated to yield the crude product, which was used without further purification.

4.1.3. General synthetic procedures for deoxybenzoins **11a–g** and **12a–d**

In a round-bottomed flask maintained under a nitrogen atmosphere, appropriate amounts of α -hydroxyphosphonate (10 mmol) and 3,4-dihydro-2H-pyran (17 mmol) as well as 1.5 mol% of *p*-TsOH·H₂O were dissolved in dry toluene (30 mL). The resulting mixture was heated to 65 °C for 2 h, and dry THF (5 mL) was then added to the mixture. Upon cooling to –55 °C, 10.5 mmol of *n*-butyllithium (15% in hexane, 1.6 mol/L) was added dropwise to the mixture, and the contents of the flask were stirred for 1 h under a nitrogen atmosphere, after which the solvent for the appropriate benzaldehyde (10 mmol) in anhydrous THF was added dropwise and stirred for another 4 h. Upon solvent removal via rotary evaporation, the residue was dissolved in a mixture of 20 mL of MeOH and HCl aq. (3 mL, 12 M) and stirred at room temperature for 1 h. Next, the flask was stored at –10 °C to allow the deoxybenzoin to precipitate as a solid. Pure product as a white solid could be obtained from this crude mixture via recrystallisation from methanol (10 mL). For example:

4.1.3.1. 1-(3,4,5-trimethoxyphenyl)-2-(naphthalen-2-yl)ethanone (11d). White solid; yield: 73%; M.p.: 68–70 °C; ¹H NMR (300 MHz, CDCl₃): δ 7.80 (m, 3H, Ph-H), 7.72 (s, 1H, Ph-H), 7.45 (m, 2H, Ph-H), 7.39 (d, *J* = 8.3 Hz, 1H, Ph-H), 7.30 (s, 2H, Ph-H), 4.40 (s, 2H, COCH₂), 3.89 (3H, s, OCH₃), 3.86 (6H, s, OCH₃). MS (ESI) *m/z* 337.2 [M + H]⁺, 359.1 [M + Na]⁺.

4.1.3.2. 1-(3,4-methylenedioxyphenyl)-2-[3-(benzyloxy)-4-methoxyphenyl]ethanone (12b). White solid; yield: 79%; M.p.: 98–101 °C; ¹H NMR (300 MHz, CDCl₃): δ 7.56 (dd, *J*₁ = 8.2 Hz, *J*₂ = 1.5 Hz, 1H, Ph-H), 7.46 (s, 2H, Ph-H), 7.42 (s, 1H, Ph-H), 7.35 (t,

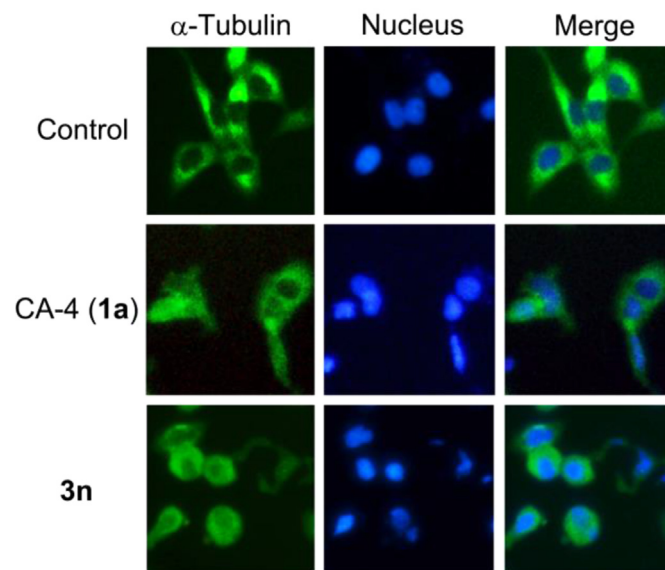


Fig. 3. CA-4 (**1a**) and compound **3n** depolymerise the microtubule network of HT-1080 cancer cells. Untreated cells (Control) and cells treated with CA-4 or compound **3n** at twice the IC₅₀ concentration for 12 h, were fixed and stained with anti- α -tubulin-FITC specific antibodies followed by DAPI. Microtubules and unassembled tubulin are shown in green, and nuclei, which were stained with DAPI, are shown in blue. (For interpretation of the references to colour in this figure legend, the reader is referred to the web version of this article.)

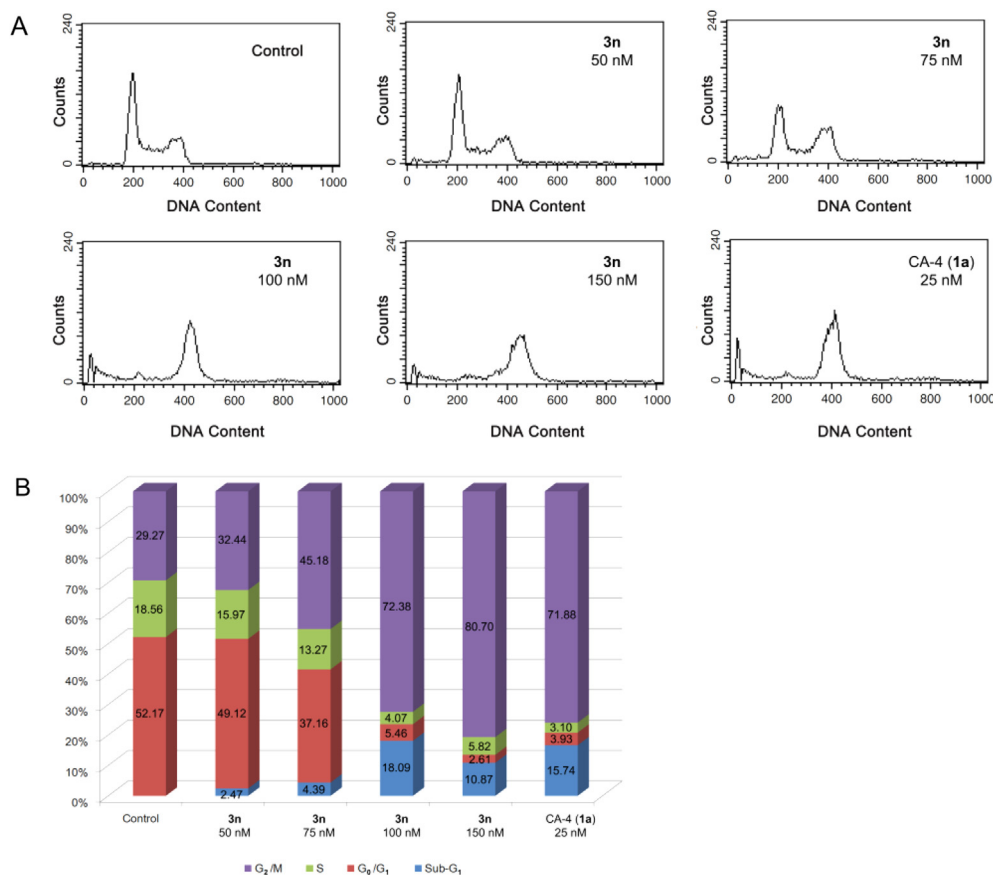


Fig. 4. Compound **3n** affects the cell cycle distribution in HT-1080 cancer cells. (A) Untreated cells (Control) and cells treated with compound **3n** at different concentrations and CA-4 at 25 nM concentration for 24 h; (B) The statistical graph of cell cycle distribution.

$J = 7.8$ Hz, 2H, Ph-H), 7.29 (m, 1H, Ph-H), 6.83 (m, 4H, Ph-H), 6.01 (s, 2H, OCH_2O), 5.11 (s, 2H, OCH_2), 4.09 (s, 2H, COCH_2), 3.85 (s, 3H, OCH_3). MS (ESI) m/z 377.3 $[\text{M} + \text{H}]^+$, 399.3 $[\text{M} + \text{Na}]^+$.

4.1.3.3. 1-(3,4-methylenedioxyphenyl)-2-(4-methoxy-3-nitrophenyl) ethanone (12c). Pale yellow solid; yield: 75%; M.p.: 143–147 °C; ^1H NMR (300 MHz, CDCl_3): δ 7.76 (s, 1H, Ph-H), 7.62 (d, $J = 8.0$ Hz, 1H, Ph-H), 7.45 (d, $J = 12.1$ Hz, 2H, Ph-H), 7.07 (d, $J = 9.0$ Hz, 1H, Ph-H), 6.88 (d, $J = 8.1$ Hz, 1H, Ph-H), 6.07 (s, 2H, OCH_2O), 4.22 (s, 2H, COCH_2), 3.96 (s, 3H, OCH_3). MS (ESI) m/z 316.2 $[\text{M} + \text{H}]^+$, 338.1 $[\text{M} + \text{Na}]^+$.

4.1.4. General synthetic procedures for benzils **13a–g** and **14a–d**

A mixture of an appropriate amount of deoxybenzoin (1 mmol) and selenium dioxide (2 mmol) in DMSO (2 mL) was placed into the MW cavity (closed vessel mode, $P_{\text{max}} = 250$ PSI). MW irradiation of 150 W was used, and the temperature was ramped from 25 to 150 °C. Once 150 °C was reached after approximately 1 min, the reaction mixture was held at this temperature for 2 min while stirring, then cooled, diluted with water, and extracted with ethyl acetate; the organic layer was washed with brine, dried over Na_2SO_4 , and filtered. The removal of the solvent yielded a residue that was purified by silica gel column chromatography (*n*-hexane:dichloromethane = 1:3 as eluent) to furnish **13a–g** and **14a–d**. For example:

4.1.4.1. 1-(Naphthalen-2-yl)-2-(3,4,5-trimethoxyphenyl)ethane-1,2-dione (13d). Pale yellow solid; yield: 71%; M.p.: 129–131 °C; ^1H NMR (300 MHz, CDCl_3): δ 8.41 (s, 1H, Ph-H), 8.10 (dd, $J_1 = 8.8$ Hz,

$J_2 = 1.8$ Hz, 1H, Ph-H), 7.94 (m, 3H, Ph-H), 7.65 (m, 1H, Ph-H), 7.57 (m, 1H, Ph-H), 7.28 (s, 2H, OCH_3), 3.96 (s, 3H, OCH_3), 3.89 (s, 6H, OCH_3). MS (ESI) m/z 351.2 $[\text{M} + \text{H}]^+$, 373.3 $[\text{M} + \text{Na}]^+$.

4.1.4.2. 1-(4-Methoxy-3-nitrophenyl)-2-(3,4-methylenedioxyphenyl) ethane-1,2-dione (14c). Orange oil; yield: 68%; ^1H NMR (300 MHz, CDCl_3): δ 8.44 (d, $J = 8.3$ Hz, 1H, Ph-H), 8.17 (dd, $J_1 = 8.9$ Hz, $J_2 = 2.3$ Hz, 1H, Ph-H), 7.50 (m, 2H, Ph-H), 7.20 (d, $J = 9.0$ Hz, 1H, Ph-H), 6.89 (d, $J = 8.0$ Hz, 1H, Ph-H), 6.10 (s, 2H, OCH_2O), 4.06 (s, 3H, OCH_3). MS (ESI) m/z 330.4 $[\text{M} + \text{H}]^+$, 352.2 $[\text{M} + \text{Na}]^+$.

4.1.5. General synthetic procedures for dioxime **15a–g** and **16a–d**

An excess of hydroxylamine hydrochloride (10 mmol) was added to a solution of an appropriate amount of benzil (1 mmol) in dry pyridine (3 mL) and ethanol (7 mL). The resulting solution was heated at 90 °C for 3 days, worked up by dilution of EtOAc and washed with HCl aq. (15 mL, 0.5 M), water (30 mL) and brine (30 mL). After drying over Na_2SO_4 and the evaporation of the solvent, the crude product was used without further purification.

4.1.6. General synthetic procedures for 3,4-diaryl-1,2,5-selenadiazoles **3a–l** and **4a–d**

A mixture of an appropriate amount of dioxime (1 mmol), selenium dioxide (1.5 mmol), and *N,N*-dimethylformamide (10 mL) was refluxed for 1 h with stirring. The reaction mixture was poured into water and extracted with EtOAc (20 mL \times 3). The combined organic layer was washed with brine and dried over Na_2SO_4 . After filtration and the evaporation of the solvent, the crude product was

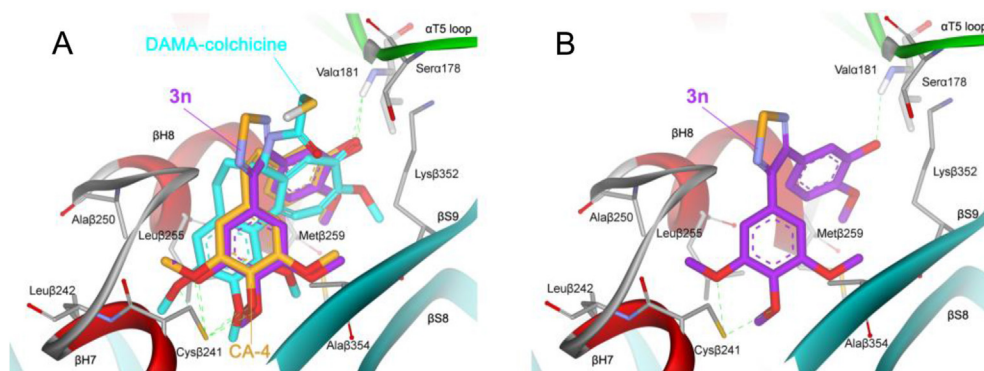


Fig. 5. (A) Predicted modes for compound **3n** (purple) and CA-4 (orange) binding in the colchicine-binding site of tubulin (PDB code: 1SA0), and overlapping with DAMA-colchicine (cyan, the native ligand of 1SA0); (B) Docking conformation of compound **3n** (purple) in the colchicine-binding site of tubulin. The dashed green lines represent hydrogen bonds, and the distance between ligands and protein is less than 2.8 Å. Surrounding amino acid side chains are shown in grey stick format and labelled. (For interpretation of the references to colour in this figure legend, the reader is referred to the web version of this article.)

purified by column chromatography (*n*-hexane: EtOAc = 10:1 as eluent) on silica gel to afford pure products.

4.1.6.1. 3-(4-methoxyphenyl)-4-(3,4,5-trimethoxyphenyl)-1,2,5-selenadiazole (3a). White solid; yield: 44%; M.p.: 94–100 °C; ¹H NMR (300 MHz, CDCl₃): δ 8.85 (d, *J* = 8.7 Hz, 2H, Ph-H), 6.86 (d, *J* = 8.7 Hz, 2H, Ph-H), 6.67 (s, 2H, Ph-H), 3.89 (s, 3H, OCH₃), 3.83 (s, 3H, OCH₃), 3.69 (s, 6H, OCH₃). ¹³C NMR (150 MHz, CDCl₃): δ 164.6, 164.3, 160.3, 152.8 (×2), 138.8, 131.2, 130.6 (×2), 128.6, 113.6 (×2), 106.5 (×2), 60.9, 55.9 (×2), 55.3; HRMS (ESI): calcd for C₁₈H₁₈N₂O₄Se [M + H]⁺: 407.0510, found: 407.0517.

4.1.6.2. 3-[3-(benzyloxy)-4-methoxyphenyl]-4-(3,4,5-trimethoxyphenyl)-1,2,5-selenadiazole (3b). White solid; yield: 47%; M.p.: 132–138 °C; ¹H NMR (300 MHz, CDCl₃): δ 7.31 (m, 5H, Ph-H), 7.04 (m, 2H, Ph-H), 6.86 (d, *J* = 18.4 Hz, 1H, Ph-H), 6.64 (s, 2H, Ph-H), 5.01 (s, 2H, OCH₂), 3.91 (s, 3H, OCH₃), 3.88 (s, 3H, OCH₃), 3.69 (s, 6H, OCH₃). ¹³C NMR (150 MHz, CDCl₃): δ 164.4, 164.4, 152.9 (×2), 150.6, 147.8, 138.9, 136.6, 131.4, 128.6, 128.5 (×2), 127.9, 127.1 (×2), 122.8, 106.5 (×2), 71.0, 60.9, 56.0, 56.0 (×2); HRMS (ESI): calcd for C₂₅H₂₄N₂O₅Se [M + H]⁺: 513.0929, found: 513.0906.

4.1.6.3. 3-(4-Methoxy-3-nitrophenyl)-4-(3,4,5-trimethoxyphenyl)-1,2,5-selenadiazole (3c). Pale yellow solid; yield: 41%; M.p.: 110–115 °C; ¹H NMR (300 MHz, CDCl₃): δ 8.09 (d, *J* = 2.2 Hz, 1H, Ph-H), 7.60 (dd, *J*₁ = 8.8 Hz, *J*₂ = 2.3 Hz, 1H, Ph-H), 7.06 (d, *J* = 8.8 Hz, 1H, Ph-H), 6.65 (s, 2H, Ph-H), 3.99 (s, 3H, OCH₃), 3.90 (s, 3H, OCH₃), 3.74 (s, 6H, OCH₃). ¹³C NMR (150 MHz, CDCl₃): δ 164.1, 161.7, 153.2 (×2), 139.4, 139.3, 134.5, 130.7, 128.4, 126.6, 113.0, 106.5 (×2), 61.0, 56.7, 56.1 (×2); HRMS (ESI): calcd for C₁₈H₁₈N₃O₆Se [M + H]⁺: 452.0361, found: 452.0317.

4.1.6.4. 3-(naphthalen-2-yl)-4-(3,4,5-trimethoxyphenyl)-1,2,5-selenadiazole (3d). White solid; yield: 48%; M.p.: 113–117 °C; ¹H NMR (300 MHz, CDCl₃): δ 8.03 (s, 1H, Ph-H), 7.82 (m, 3H, Ph-H), 7.51 (m, 3H, Ph-H), 6.69 (s, 2H, Ph-H), 3.86 (s, 3H, OCH₃), 3.54 (s, 6H, OCH₃). ¹³C NMR (150 MHz, CDCl₃): δ 164.8, 164.5, 152.9 (×2), 139.0, 133.6, 133.2, 132.8, 130.9, 129.1, 128.3, 127.8, 127.6, 127.0, 126.6, 126.2, 106.6 (×2), 60.9, 55.8 (×2); HRMS (ESI): calcd for C₂₁H₁₉N₂O₃Se [M + H]⁺, C₂₁H₁₈N₂O₃Se [M + Na]⁺: 427.0561, 449.0380, found: 427.0590, 449.0376.

4.1.6.5. 3-[3-(benzyloxy)phenyl]-4-(3,4,5-trimethoxyphenyl)-1,2,5-selenadiazole (3e). Oil; yield: 45%; ¹H NMR (300 MHz, CDCl₃): δ 7.35 (m, 5H, Ph-H), 7.26 (m, 1H, Ph-H), 7.10 (m, 1H, Ph-H), 6.66 (s, 2H, Ph-

H), 5.01 (s, 2H, PhCH₂), 3.87 (s, 3H, OCH₃), 3.65 (s, 6H, OCH₃). ¹³C NMR (150 MHz, CDCl₃): δ 164.6, 164.2, 152.9 (×2), 136.6, 128.6 (×2), 128.1, 127.3 (×2), 121.9, 116.2, 115.5, 106.6 (×2), 70.1, 60.9, 56.0 (×2). MS (ESI): *m/z* 483.2 [M + H]⁺, 505.2 [M + Na]⁺.

4.1.6.6. 3-(4-ethoxyphenyl)-4-(3,4,5-trimethoxyphenyl)-1,2,5-selenadiazole (3i). White solid; yield: 44%; M.p.: 139–143 °C; ¹H NMR (300 MHz, CDCl₃): δ 7.39 (d, *J* = 8.7 Hz, 2H, Ph-H), 6.88 (d, *J* = 8.7 Hz, 2H, Ph-H), 6.67 (s, 2H, Ph-H), 4.05 (q, *J* = 7.0 Hz, 2H, OCH₂CH₃), 3.89 (s, 3H, OCH₃), 3.69 (s, 6H, OCH₃), 1.43 (t, *J* = 7.0 Hz, 3H, OCH₂CH₃). ¹³C NMR (150 MHz, CDCl₃): δ 164.6, 164.3, 159.6, 152.8 (×2), 138.8, 131.3, 130.6 (×2), 128.5, 114.1 (×2), 106.5 (×2), 63.5, 60.8, 55.9 (×2), 14.6; HRMS (ESI): calcd for C₁₉H₂₁N₂O₄Se [M + H]⁺, C₁₉H₂₀N₂NaO₄Se [M + Na]⁺: 421.0667, 443.0486, found: 421.0687, 443.0482.

4.1.6.7. 3-(3-bromo-4-methoxyphenyl)-4-(3,4,5-trimethoxyphenyl)-1,2,5-selenadiazole (3j). White solid; yield: 39%; M.p.: 103–108 °C; ¹H NMR (300 MHz, CDCl₃): δ 7.78 (d, *J* = 1.9 Hz, 1H, Ph-H), 7.31 (dd, *J*₁ = 8.7 Hz, *J*₂ = 1.9 Hz, 1H, Ph-H), 6.85 (d, *J* = 8.7 Hz, 1H, Ph-H), 6.67 (s, 2H, Ph-H), 3.92 (s, 3H, OCH₃), 3.89 (s, 3H, OCH₃), 3.72 (s, 6H, OCH₃). ¹³C NMR (150 MHz, CDCl₃): δ 164.2, 162.9, 156.6, 153.0 (×2), 139.1, 134.2, 131.0, 129.7, 129.5, 111.1, 106.6 (×2), 60.9, 56.3, 56.0 (×2); HRMS (ESI): calcd for C₁₈H₁₈BrN₂O₄Se [M + H]⁺, C₁₈H₁₇BrN₂NaO₄Se [M + Na]⁺: 484.9615, 506.9435, found: 484.9617, 506.9429.

4.1.6.8. 3-(3-bromo-4-ethoxyphenyl)-4-(3,4,5-trimethoxyphenyl)-1,2,5-selenadiazole (3k). White solid; yield: 42%; M.p.: 113–115 °C; ¹H NMR (300 MHz, CDCl₃): δ 7.77 (d, *J* = 1.9 Hz, 1H, Ph-H), 7.27 (dd, *J*₁ = 8.4 Hz, *J*₂ = 1.9 Hz, 1H, Ph-H), 6.82 (d, *J* = 8.4 Hz, 1H, Ph-H), 6.66 (s, 2H, Ph-H), 4.11 (q, *J* = 6.9 Hz, 2H, OCH₂CH₃), 3.87 (s, 3H, OCH₃), 3.72 (s, 6H, OCH₃), 1.48 (t, *J* = 6.8 Hz, 3H, OCH₂CH₃). ¹³C NMR (150 MHz, CDCl₃): δ 164.1, 162.9, 156.0, 152.9 (×2), 139.1, 134.2, 131.0, 129.5, 129.4, 112.1, 111.8, 106.6 (×2), 64.8, 60.9, 56.0 (×2), 14.5; HRMS (ESI): calcd for C₁₉H₂₀BrN₂O₄Se [M + H]⁺, C₁₉H₁₉BrN₂NaO₄Se [M + Na]⁺: 498.9772, 520.9591, found: 498.9746, 520.9572.

4.1.6.9. 3-(4-bromophenyl)-4-(3,4,5-trimethoxyphenyl)-1,2,5-selenadiazole (3l). White solid; yield: 40%; M.p.: 112–115 °C; ¹H NMR (300 MHz, CDCl₃): δ 7.52 (d, *J* = 8.4 Hz, 2H, Ph-H), 7.35 (d, *J* = 8.4 Hz, 2H, Ph-H), 6.62 (s, 2H, Ph-H), 3.89 (s, 3H, OCH₃), 3.69 (s, 6H, OCH₃). ¹³C NMR (150 MHz, CDCl₃): δ 164.3, 163.6, 153.0 (×2), 139.1, 135.1, 131.5 (×2), 130.7 (×2), 130.7, 123.7, 106.5 (×2), 60.9, 55.9 (×2); HRMS (ESI): calcd for C₁₇H₁₆BrN₂O₃Se [M + H]⁺,

$C_{17}H_{15}BrN_2NaO_3Se$ [M + Na]⁺: 454.9510, 476.9329, found: 454.9502, 476.9277.

4.1.6.10. 3-(4-methoxyphenyl)-4-(3,4-methylenedioxyphenyl)-1,2,5-selenadiazole (**4a**). White solid; yield: 46%; M.p.: 98–101 °C; ¹H NMR (300 MHz, CDCl₃): δ 7.39 (m, 2H, Ph-H), 6.89 (m, 4H, Ph-H), 6.76 (d, J = 8.0 Hz, 1H, Ph-H), 5.99 (s, 2H, OCH₂O), 3.83 (s, 3H, OCH₃); ¹³C NMR (150 MHz, CDCl₃): δ 164.7, 164.3, 156.1, 152.7 (×2), 138.8, 137.5, 130.7 (×2), 129.6, 121.2 (×2), 116.5, 116.1, 106.6, 55.9; HRMS (ESI): calcd for C₁₆H₁₃N₂O₃Se [M + H]⁺: 361.0091, found: 361.0086.

4.1.6.11. 3-(4-methoxy-3-nitrophenyl)-4-(3,4-methylenedioxyphenyl)-1,2,5-selenadiazole (**4c**). Brown solid; yield: 44%; M.p.: 58–63 °C; ¹H NMR (300 MHz, CDCl₃): δ 8.01 (d, J = 2.3 Hz, 1H, Ph-H), 7.63 (dd, J₁ = 8.8 Hz, J₂ = 2.3 Hz, 1H, Ph-H), 7.06 (d, J = 8.8 Hz, 1H, Ph-H), 6.92 (d, J = 1.6 Hz, 1H, Ph-H), 6.87 (dd, J₁ = 7.9 Hz, J₂ = 1.6 Hz, 1H, Ph-H), 6.80 (d, J = 7.9 Hz, 1H, Ph-H), 6.02 (s, 2H, OCH₂O), 4.00 (s, 3H, OCH₃); ¹³C NMR (150 MHz, CDCl₃): δ 164.0, 161.7, 153.4, 148.8, 147.9, 139.3, 134.6, 129.3, 128.4, 126.6, 123.4, 113.2, 109.4, 108.4, 101.5, 56.6; HRMS (ESI): calcd for C₁₆H₁₂N₃O₅Se [M + H]⁺, C₁₆H₁₁N₃NaO₅Se [M + Na]⁺: 405.9942, 427.9762, found: 405.9905, 427.9740.

4.1.6.12. 3-(naphthalen-2-yl)-4-(3,4-methylenedioxyphenyl)-1,2,5-selenadiazole (**4d**). White solid; yield: 47%; M.p.: 138–142 °C; ¹H NMR (300 MHz, CDCl₃): δ 8.03 (s, 1H, Ph-H), 7.83 (m, 3H, Ph-H), 7.51 (m, 3H, Ph-H), 6.99 (d, J = 1.4 Hz, 1H, Ph-H), 6.89 (dd, J₁ = 8.0 Hz, J₂ = 1.4 Hz, 1H, Ph-H), 6.71 (d, J = 8.0 Hz, 1H, Ph-H), 5.98 (s, 2H, OCH₂O); ¹³C NMR (150 MHz, CDCl₃): δ 164.7, 164.4, 148.5, 147.6, 133.5, 133.3, 132.9, 129.8, 129.0, 128.4, 127.9, 127.7, 126.9, 126.5, 126.2, 123.6, 109.6, 108.1, 101.3; HRMS (ESI): calcd for C₁₉H₁₂N₂O₄Se [M + H]⁺: 381.0142, found: 381.0124.

4.1.7. General synthetic procedures for compounds **3m–p** and **4n**

AlCl₃ (1.5 mmol) was added in one portion to a solution of compound **3b**, **3e**, **3f**, **3g** or **4b** (0.5 mmol) in CH₂Cl₂ (25 mL) at 0 °C. When the reaction was completed (TLC control), the mixture was poured into water (50 mL)/HCl aq. (50 mL, 2 M) and extracted with CH₂Cl₂ (20 mL × 3). The combined organic layers were washed with water, dried over Na₂SO₄, and the solvent was then evaporated under reduced pressure. The residue was purified by silica gel chromatography to afford pure product.

4.1.7.1. 3-(3-hydroxyphenyl)-4-(3,4,5-trimethoxyphenyl)-1,2,5-selenadiazole (**3m**). White solid; yield: 87%; M.p.: 125–130 °C; ¹H NMR (300 MHz, CDCl₃): δ 7.20 (t, J = 8.0 Hz, 1H, Ph-H), 6.93 (d, J = 7.1 Hz, 2H, Ph-H), 6.87 (dd, J₁ = 8.3 Hz, J₂ = 2.1 Hz, 1H, Ph-H), 6.68 (s, 2H, Ph-H), 3.86 (s, 3H, OCH₃), 3.65 (s, 6H, OCH₃); ¹³C NMR (150 MHz, CDCl₃): δ 168.0, 164.4, 164.2, 160.3 (×2), 148.4, 147.5, 130.50, 123.5, 113.7, 109.5, 108.1, 101.3 (×2), 55.2 (×2), 52.6; HRMS (ESI): calcd for C₁₇H₁₇N₂O₄Se [M + H]⁺, C₁₇H₁₆N₂NaO₄Se [M + Na]⁺: 393.0354, 415.0173, found: 393.0329, 415.0213.

4.1.7.2. 3-(3-hydroxy-4-methoxyphenyl)-4-(3,4,5-trimethoxyphenyl)-1,2,5-selenadiazole (**3n**). White solid; yield: 84%; M.p.: 115–118 °C; ¹H NMR (300 MHz, CDCl₃): δ 7.10 (d, J = 2.0 Hz, 1H, Ph-H), 6.91 (dd, J₁ = 8.4 Hz, J₂ = 2.0 Hz, 1H, Ph-H), 6.82 (d, J = 8.4 Hz, 1H, Ph-H), 6.69 (s, 2H, Ph-H), 5.80 (s, 1H, Ph-OH), 3.91 (s, 3H, OCH₃), 3.88 (s, 3H, OCH₃), 3.70 (s, 6H, OCH₃); ¹³C NMR (150 MHz, CDCl₃): δ 164.5, 164.4, 152.9 (×2), 147.5, 145.4, 139.0, 131.2, 129.5, 121.5, 115.6, 110.1, 106.6 (×2), 60.9, 56.0 (×2), 53.4; HRMS (ESI): calcd for C₁₈H₁₉N₂O₅Se [M + H]⁺, C₁₈H₁₈N₂NaO₅Se [M + Na]⁺: 423.0459, 445.0279, found: 423.0463, 445.0269.

4.1.7.3. 3-(4-hydroxyphenyl)-4-(3,4,5-trimethoxyphenyl)-1,2,5-selenadiazole (**3o**). White solid; yield: 85%; M.p.: 190–195 °C; ¹H NMR (300 MHz, DMSO-*d*₆): δ 7.21 (d, J = 8.5 Hz, 2H, Ph-H), 6.78 (d, J = 8.6 Hz, 2H, Ph-H), 6.66 (s, 2H, Ph-H), 5.75 (s, 1H, Ph-OH), 3.69 (s, 3H, OCH₃), 3.60 (s, 6H, OCH₃); ¹³C NMR (150 MHz, CDCl₃): δ 164.8, 164.4, 157.1, 152.9 (×2), 138.8, 131.3, 130.8 (×2), 128.4, 115.2 (×2), 106.6 (×2), 61.0, 55.9 (×2); HRMS (ESI): calcd for C₁₇H₁₇N₂O₄Se [M + H]⁺, C₁₇H₁₆N₂NaO₄Se [M + Na]⁺: 393.0354, 415.0173, found: 393.0331, 415.0159.

4.1.7.4. 3-(3-bromo-4-hydroxyphenyl)-4-(3,4,5-trimethoxyphenyl)-1,2,5-selenadiazole (**3p**). White solid; yield: 81%; M.p.: 148–153 °C; ¹H NMR (300 MHz, CDCl₃): δ 7.69 (d, J = 2.0 Hz, 1H, Ph-H), 7.27 (dd, J₁ = 8.4 Hz, J₂ = 2.1 Hz, 1H, Ph-H), 6.97 (d, J = 8.5 Hz, 1H, Ph-H), 6.68 (s, 2H, Ph-H), 5.91 (s, 1H, Ph-OH), 3.89 (s, 3H, OCH₃), 3.72 (s, 6H, OCH₃); ¹³C NMR (150 MHz, CDCl₃): δ 164.2, 162.9, 153.4, 153.0 (×2), 139.2, 133.2, 130.9, 130.1, 129.8, 115.7, 110.0, 106.6 (×2), 61.0, 56.1 (×2); HRMS (ESI): calcd for C₁₇H₁₆BrN₂O₄Se [M + H]⁺, C₁₇H₁₅BrN₂NaO₄Se [M + Na]⁺: 470.9459, 492.9278, found: 470.9441, 492.9276.

4.1.7.5. 3-(3-hydroxy-4-methoxyphenyl)-4-(3,4-methylenedioxyphenyl)-1,2,5-selenadiazole (**4n**). White solid; yield: 86%; M.p.: 89–94 °C; ¹H NMR (300 MHz, CDCl₃): δ 7.03 (d, J = 2.1 Hz, 1H, Ph-H), 6.93 (m, 3H, Ph-H), 6.79 (q, J = 8.3 Hz, 2H, Ph-H), 5.99 (s, 2H, OCH₂O), 3.91 (s, 3H, OCH₃); ¹³C NMR (150 MHz, CDCl₃): δ 164.3, 164.2, 148.4, 147.5 (×2), 145.3, 130.0, 129.4, 123.6, 121.5, 115.4, 110.2, 109.6, 108.1, 101.3, 55.9; HRMS (ESI): calcd for C₁₆H₁₃N₂O₄Se [M + H]⁺: 377.0041, found: 377.0027.

4.1.8. General synthetic procedures for compounds **3q**, **3r** and **4q**

The compound **3c**, **3h** or **4c** (0.5 mmol) was slowly mixed with an Fe(OH)₂ solution [treatment of FeSO₄ (5.0 mmol) in H₂O (15 mL) with a cone. NH₄OH solution (5 mL)] and refluxed for 30 min. Following addition of warm H₂O (10 mL), the mixture was filtered, the precipitate washed with warm H₂O (10 mL) and the combined filtrates acidified with 3 N H₂SO₄. Extraction of the resultant solution with EtOAc (20 mL × 3) and evaporation of the solvent yielded the crude product, purified by column chromatography (*n*-hexane: EtOAc = 10:1 as eluent) on silica gel to afford pure products.

4.1.8.1. 3-(3-amino-4-methoxyphenyl)-4-(3,4,5-trimethoxyphenyl)-1,2,5-selenadiazole (**3q**). Brown solid; yield: 77%; M.p.: 116–119 °C; ¹H NMR (300 MHz, CDCl₃): δ 6.89 (s, 1H, Ph-H), 6.72 (d, 4H, Ph-H), 3.88 (s, 3H, OCH₃), 3.87 (s, 3H, OCH₃), 3.71 (s, 6H, OCH₃); ¹³C NMR (150 MHz, CDCl₃): δ 165.0, 164.4, 152.8 (×2), 148.1, 138.9, 136.0, 131.4, 129.0, 119.9, 115.5, 109.7, 106.6 (×2), 60.9, 56.0 (×2), 55.6; HRMS (ESI): calcd for C₁₈H₂₀N₃O₄Se [M + H]⁺, C₁₈H₁₉N₃NaO₄Se [M + Na]⁺: 422.0619, 444.0438, found: 422.0606, 444.0373.

4.1.8.2. 3-(3-amino-4-ethoxyphenyl)-4-(3,4,5-trimethoxyphenyl)-1,2,5-selenadiazole (**3r**). Brown solid; yield: 83%; M.p.: 97–101 °C; ¹H NMR (300 MHz, CDCl₃): δ 6.90 (s, 1H, Ph-H), 6.71 (d, 4H, Ph-H), 4.07 (q, J = 7.0 Hz, 2H, OCH₂CH₃), 3.88 (s, 3H, OCH₃), 3.71 (s, 6H, OCH₃), 1.44 (t, J = 7.0 Hz, 3H, OCH₂CH₃); ¹³C NMR (150 MHz, CDCl₃): δ 165.1, 164.4, 152.8 (×2), 147.4, 138.9, 136.1, 131.4, 128.9, 119.8, 115.6, 110.6, 106.6 (×2), 63.9, 60.9, 56.0 (×2), 14.8; HRMS (ESI): calcd for C₁₉H₂₂N₃O₄Se [M + H]⁺, C₁₉H₂₁N₃NaO₄Se [M + Na]⁺: 436.0776, 458.0595, found: 436.0770, 458.0594.

4.1.8.3. 3-(3-amino-4-methoxyphenyl)-4-(3,4-methylenedioxyphenyl)-1,2,5-selenadiazole (**4q**). Brown solid; yield: 85%; M.p.: 71–78 °C; ¹H NMR (300 MHz, CDCl₃): δ 6.97 (d, J = 1.6 Hz, 1H, Ph-H), 6.93 (dd, J₁ = 8.0 Hz, J₂ = 1.7 Hz, 1H, Ph-H), 6.87 (s, 1H, Ph-H), 6.75 (m, 3H, Ph-H), 5.99 (s, 2H, OCH₂O), 3.87 (s, 3H,

OCH₃); ¹³C NMR (150 MHz, CDCl₃): δ 164.9, 164.3, 148.4, 148.2, 147.4, 136.0, 130.3, 128.9, 123.6, 119.8, 115.5, 109.8, 109.6, 108.1, 101.3, 55.5; HRMS (ESI): calcd for C₁₆H₁₄N₃O₃Se [M + H]⁺: 376.0200, found: 376.0197.

4.1.9. 3-[3-(N-methylamino)-4-methoxyphenyl]-4-(3,4,5-trimethoxyphenyl)-1,2,5-selenadiazole (**3s**)

To a solution of iodomethane (0.002 mol) in DMF (5 mL) was added dropwise the solution of compound **3q** (0.002 mmol) in DMF (0.5 mL) and the mixture was heated under stirring at 40 °C for 24 h. The reaction was diluted with H₂O (100 mL) then extracted with EtOAc (3 × 100 mL) and the combined organic phases were washed with H₂O (3 × 100 mL) and brine (50 mL), dried over Na₂SO₄ and concentrated in vacuo. The residue was purified by flash column chromatography (*n*-hexane: EtOAc = 10:1 as eluent). Brown solid; yield: 92%; M.p.: 119–123 °C; ¹H NMR (300 MHz, CDCl₃): δ 6.71 (m, 5H, Ph-H), 4.68 (s, 1H, NHCH₃), 3.87 (s, 3H, OCH₃), 3.86 (s, 3H, OCH₃), 3.70 (s, 6H, OCH₃), 2.75 (s, 3H, NHCH₃). ¹³C NMR (150 MHz, CDCl₃): δ 165.6, 164.6, 152.8 (×2), 147.7, 139.0, 138.8, 131.7, 129.1, 117.9, 110.1, 108.5, 106.7 (×2), 60.9, 56.0 (×2), 55.5, 30.2; HRMS (ESI): calcd for C₁₉H₂₂N₃O₄Se [M + H]⁺, C₁₉H₂₁N₃NaO₄Se [M + Na]⁺: 436.0776, 458.0595, found: 436.0772, 458.0530.

4.2. Biological evaluation

4.2.1. Cell culture

The human gastric adenocarcinoma cell line SGC-7901, the human fibrosarcoma cell line HT-1080 and the human pulmonary carcinoma cell line A-549 were cultured in RPMI-1640 medium containing 10% FBS, 100 U/mL streptomycin and 100 U/mL penicillin at 37 °C in a humidified atmosphere containing 5% CO₂. All cell lines were purchased from the American Type Culture Collection (ATCC, Manassas, VA).

4.2.2. In vitro anti-proliferative activity

The *in vitro* anti-proliferative activities of CA-4 (**1a**) and all of the target compounds were determined with an MTT (Sigma) assay. Briefly, cells were seeded into 96-well plates at a density of 1–3 × 10⁴/well (depending on the cell growth rate). Twenty-four hours later, triplicate wells were treated with media and the agents. After 72 h of incubation at 37 °C in 5% CO₂, the drug-containing medium was removed and replaced with 100 μL of fresh medium containing 5 mg/mL MTT solution. After 4 h of incubation, the medium with MTT was removed, and 100 μL of dimethyl sulphoxide (DMSO) was added to each well. The plates were gently agitated until the purple formazan crystals were dissolved, and the OD₄₉₀ was determined using a microplate reader (MK3, Thermo, Germany). The data were calculated and plotted as the per cent viability compared to the control. The 50% inhibitory concentration (IC₅₀) was defined as the concentration that reduced the absorbance of the untreated wells by 50% of the vehicle in the MTT assay.

4.2.3. Inhibition of tubulin polymerisation

The effects of compounds **3n** and CA-4 (**1a**) on the polymerisation of tubulin were determined by employing a fluorescence-based tubulin polymerisation assay kit (Cytoskeleton-Cat.# BK011P) according to the manufacturer's protocol. Tubulin was re-suspended in ice-cold G-PEM buffer (80 mM PIPES, 2 mM MgCl₂, 0.5 mM EGTA, 1 mM GTP, 20% (v/v) glycerol) and added to wells on a 96-well plate containing the designated concentration of the drug or vehicle. The samples were mixed well, and tubulin assembly was monitored (emission wavelength of 420 nm; excitation wavelength of 360 nm) at 1 min intervals for 90 min at 37 °C using a plate

reader (FASCalibur, BD Biosciences, USA). The IC₅₀ values were calculated after 20 min using the SPSS software.

4.2.4. Immunofluorescence staining

Immunostaining was carried out to detect the microtubule-associated tubulin protein after exposure to CA-4 (**1a**) and the investigated compound **3n**. HT-1080 cells were seeded at 1 × 10⁴ cells per well on a 24-well plate and grown for 24 h. The cells were treated with the vehicle or twice the IC₅₀ concentration of CA-4 (**1a**) or **3n** for 12 h. The control and treated cells were fixed with 4% formaldehyde in PBS for 30 min at –20 °C, washed twice with PBS and permeabilised with 0.1% (v/v) Triton X-100 in PBS for 5 min. The cells were then blocked with 5% bovine serum albumin (BSA) in PBS for 10 min. The primary α-tubulin antibody (Santa Cruz, CA) was diluted (1:100) with 2% BSA in PBS and incubated overnight at 4 °C. The cells were washed with PBS to remove unbound primary antibody, and the cells were then incubated with FITC-conjugated antimouse secondary antibody and diluted (1:1000) with 2% BSA in PBS for 3 h at 37 °C. The cells were washed with PBS to remove unbound secondary antibody, the nuclei were stained with 4,6-diamino-2-phenolindol dihydrochloride (DAPI) and immunofluorescence was then detected using a fluorescence microscope (Olympus, Tokyo, Japan).

4.2.5. Cell cycle analysis

HT-1080 cells (8 × 10⁴ cells) were incubated with various concentrations of CA-4 (**1a**), **3n** or 0.05% DMSO for the indicated times. The cells were collected by centrifugation, washed with PBS and fixed in ice-cold 70% ethanol. The fixed cells were harvested by centrifugation and resuspended in 500 μL of PBS containing 1 mg/mL RNase. After 30 min of incubation at 37 °C, the cells were stained with 50 μg/mL propidium iodide (PI) at 4 °C in the dark for 30 min. The samples were then analysed by FACSscan flow cytometry (Becton–Dickinson, Franklin Lakes, NJ, USA). The experiments were repeated at least three times.

4.3. Molecular modelling

The molecular modelling studies were performed with Accelrys Discovery Studio 3.0. The crystal structure of tubulin complexed with DAMA-colchicine (PDB: 1SA0) was retrieved from the RCSB Protein Data Bank (<http://www.rcsb.org/pdb>). In the docking process, the protein protocol was prepared via several operations, including the standardisation of atom names, insertion of missing atoms in residues and removal of alternate conformations, insertion of missing loop regions based on SEQRES data, optimisation of short and medium sized loop regions with the Loooper Algorithm, minimisation of remaining loop regions, calculation of pK, and protonation of the structure. The receptor model was then typed with the CHARMM force field, and a binding sphere with radius of 9.0 Å was defined with the original ligand (DAMA-colchicine) as the binding site. The CA-4 (**1a**) and **3n** were drawn with Chemdraw and fully minimised using the CHARMM force field. Finally, they were docked into the binding site using the CDOCKER protocol with the default settings.

Acknowledgements

We gratefully acknowledge the National S&T Major Project (2012ZX09103101-060), the National Natural Science Foundation of China (30973614), and the Excellent Talent Supporting Project of Liaoning Province (LR20013046) for their generous financial support. This work was also supported by the Program for Innovative Research Team of the Ministry of Education and Program for Liaoning Innovative Research Team in University.

Appendix A. Supplementary data

Supplementary data associated with this article can be found in the online version, at <http://dx.doi.org/10.1016/j.ejmech.2014.09.046>. These data include MOL files and InChIKeys of the most important compounds described in this article.

References

- [1] L.B. Salum, W.F. Altei, L.D. Chiaradia, M.N.S. Cordeiro, R.R. Canevarolo, C.P.S. Melo, E. Winter, B. Mattei, H.N. Daghestani, M.C. Santos-Silva, T.B. Creczynski-Pasa, R.A. Yunes, J.A. Yunes, A.D. Andricopulo, B.W. Day, R.J. Nunes, A. Vogt, Cytotoxic 3,4,5-trimethoxychalcones as mitotic arresters and cell migration inhibitors, *Eur. J. Med. Chem.* 63 (2013) 501–510.
- [2] K.H. Downing, E. Nogales, Tubulin and microtubule structure, *Curr. Opin. Cell Biol.* 10 (1998) 16–22.
- [3] A. Wienecke, G. Bacher, Indibulin, a novel microtubule inhibitor, discriminates between mature neuronal and nonneuronal tubulin, *Cancer Res.* 69 (2009) 171–177.
- [4] M.A. Jordan, L. Wilson, Microtubules as a target for anticancer drugs, *Nat. Rev. Cancer* 4 (2004) 253–265.
- [5] C. Dumontet, M.A. Jordan, Microtubule-binding agents: a dynamic field of cancer therapeutics, *Nat. Rev. Drug. Discov.* 9 (2010) 790–803.
- [6] Y. Lu, J. Chen, M. Xiao, W. Li, D.D. Miller, An overview of tubulin inhibitors that interact with the colchicine binding site, *Pharm. Res.* 29 (2012) 2943–2971.
- [7] G.R. Pettit, S.B. Singh, E. Hamel, C.M. Lin, D.S. Alberts, D. Garcia-Kendall, Isolation and structure of the strong cell growth and tubulin inhibitor combretastatin A-4, *Experientia* 45 (1989) 209–211.
- [8] G.R. Pettit, S.B. Singh, M.R. Boyd, E. Hamel, R.K. Pettit, J.M. Schmidt, F. Hogan, Antineoplastic agents. 291. Isolation and synthesis of combretastatins A-4, A-5, and A-6(1a), *J. Med. Chem.* 38 (1995) 1666–1672.
- [9] J. Zhou, J. Jin, Y. Zhang, Y. Yin, X. Chen, B. Xu, Synthesis and antiproliferative evaluation of novel benzoimidazole-contained oxazole-bridged analogs of combretastatin A-4, *Eur. J. Med. Chem.* 68 (2013) 222–232.
- [10] Z.Y. Liu, Y.M. Wang, Y.X. Han, L. Liu, J. Jin, H. Yi, Z.R. Li, J.D. Jiang, D.W. Boykin, Synthesis and antitumor activity of novel 3,4-diaryl squaric acid analogs, *Eur. J. Med. Chem.* 65 (2013) 187–194.
- [11] R. Romagnoli, P.G. Baraldi, M.D. Carrion, O. Cruz-Lopez, M. Tolomeo, S. Grimaudo, A.D. Cristina, M.R. Pipitone, J. Balzarini, A. Brancale, E. Hamel, Substituted 2-(3',4',5'-trimethoxybenzoyl)-benzo[b]thiophene derivatives as potent tubulin polymerization inhibitors, *Bioorg. Med. Chem.* 18 (2010) 5114–5122.
- [12] Z.Y. Liu, Y.M. Wang, Z.R. Li, J.D. Jiang, D.W. Boykin, Synthesis and anticancer activity of novel 3,4-diarylthiazol-2(3H)-ones (imines), *Bioorg. Med. Chem. Lett.* 19 (2009) 5661–5664.
- [13] M.K. Gurjar, R.D. Wakharkar, A.T. Singh, M. Jaggi, H.B. Borate, P.D. Shinde, R. Verma, P. Rajendran, S. Dutt, G. Singh, V.K. Sanna, M.K. Singh, S.K. Srivastava, V.A. Mahajan, V.H. Jadhav, K. Dutta, K. Krishnan, A. Chaudhary, S.K. Agarwal, R. Mukherjee, A.C. Burman, Synthesis and evaluation of 4/5-hydroxy-2,3-diaryl(substituted)-cyclopent-2-en-1-ones as cis-restricted analogues of combretastatin A-4 as novel anticancer agents, *J. Med. Chem.* 50 (2007) 1744–1753.
- [14] M. Wu, Q. Sun, C. Yang, D. Chen, J. Ding, Y. Chen, L. Lin, Y. Xie, Synthesis and activity of combretastatin A-4 analogues: 1,2,3-thiadiazoles as potent anti-tumor agents, *Bioorg. Med. Chem. Lett.* 17 (2007) 869–873.
- [15] G.C. Tron, F. Pagliai, E.D. Grosso, A.A. Genazzani, G. Sorba, Synthesis and cytotoxic evaluation of combretastatins, *J. Med. Chem.* 48 (2005) 3260–3268.
- [16] E. Moreno, D. Plano, I. Lamberto, M. Font, I. Encío, J.A. Palop, C. Sanmartín, Sulfur and selenium derivatives of quinazoline and pyrido[2,3-d]pyrimidine: synthesis and study of their potential cytotoxic activity in vitro, *Eur. J. Med. Chem.* 47 (2012) 283–298.
- [17] E. Domínguez-Álvarez, D. Plano, M. Font, A. Calvo, C. Prior, C. Jacob, J.A. Palop, C. Sanmartín, Synthesis and antiproliferative activity of novel selenoester derivatives, *Eur. J. Med. Chem.* 73 (2014) 153–166.
- [18] M.A. Fernández-Herrera, J. Sandoval-Ramírez, L. Sánchez-Sánchez, H. López-Muñoz, M.L. Escobar-Sánchez, Probing the selective antitumor activity of 22-oxo-26-selenocyanocholestane derivatives, *Eur. J. Med. Chem.* 74 (2014) 451–460.
- [19] G. Mugesh, W.W.D. Mont, H. Sies, Chemistry of biologically important synthetic organoselenium compounds, *Chem. Rev.* 101 (2001) 2125–2179.
- [20] E. Napolitano, R. Fiaschi, Marsili, α -Aryl- α -(2-tetrahydropyran-2-yl)oxy)methanephosphonates as reagents in the Horner reaction. A simple novel synthesis of (\pm)-combretastatin, *Gazz. Chim. Ital.* 118 (1988) 415–416.
- [21] G.L. Regina, T. Sarkar, R.L. Bai, M.C. Edler, R. Saletti, A. Coluccia, F. Piscitelli, L. Minelli, V. Gatti, C. Mazzoccoli, V. Palermo, C. Mazzoni, C. Falcone, A.I. Scovassi, V. Giansanti, P. Campiglia, A. Porta, B. Maresca, E. Hamel, A. Brancale, E. Novellino, R. Silvestri, New arylthioindoles and related bioisosteres at the sulfur bridging group. 4. Synthesis, tubulin polymerization, cell growth inhibition, and molecular modeling studies, *J. Med. Chem.* 52 (2009) 7512–7527.
- [22] Vincenzo Bertini, 1,2,5-selenadiazoles, *Gazz. Chim. Ital.* 97 (1967) 1870–1884.
- [23] H.C. Nickel, P. Schmidt, K.J. Böhm, S. Baasner, K. Müller, M. Gerlach, E. Unger, E.G. Günther, H. Prinz, Synthesis, antiproliferative activity and inhibition of tubulin polymerization by 1,5- and 1,8-disubstituted 10H-anthracen-9-ones bearing a 10-benzylidene or 10-(2-oxo-2-phenylethylidene) moiety, *Eur. J. Med. Chem.* 45 (2010) 3420–3438.
- [24] A.P.N. Burger, E.V. Brandt, D.G. Roux, O-(dihydrobenzofuranyl)-dibenzo- α -pyrones from *Umtiza listerana*, *Phytochemistry* 22 (1983) 2813–2817.
- [25] R.B.G. Ravelli, B. Gigant, P.A. Curmi, I. Jourdain, S. Lachkar, A. Sobel, M. Knossow, Insight into tubulin regulation from a complex with colchicine and a stathmin-like domain, *Nature* 428 (2004) 198–202.
- [26] A. Dorléans, B. Gigant, R.B.G. Ravelli, P. Mailliet, V. Mikol, M. Knossow, Variations in the colchicine-binding domain provide insight into the structural switch of tubulin, *Proc. Natl. Acad. Sci. U. S. A.* 106 (2009) 13775–13779.